

Effect of size of TiO₂ nanoparticles applied onto glass slide and porcine skin on generation of free radicals under ultraviolet irradiation

Alexey P. Popov

University of Oulu and Infotech Oulu
Faculty of Technology
Department of Electrical Engineering
Optoelectronics and Measurement Techniques
Laboratory
P.O. Box 4500
FI-90014 Oulu, Finland
and
M. V. Lomonosov Moscow State University
International Laser Center
Leninskie Gory
119991 Moscow, Russia

Stefan Haag

Martina Meinke

Jürgen Lademann

Charité-Universitätsmedizin Berlin
Department of Dermatology and Allergology
Center of Applied Cutaneous Physiology
Charitéplatz 1
D-10117 Berlin, Germany

Alexander V. Priezzhev

M. V. Lomonosov Moscow State University
Physics Department and International Laser Center
Leninskie Gory
119991 Moscow, Russia

Risto Myllylä

University of Oulu and Infotech Oulu
Faculty of Technology
Department of Electrical Engineering
Optoelectronics and Measurement Techniques
Laboratory
P.O. Box 4500
FI-90014 Oulu, Finland

1 Introduction

Free radicals are molecular species with an unpaired electron on the external orbital and of high chemical reactivity. All radicals existing in a human organism can be divided into two kinds, natural and alien. The former are those which are inherently produced in the organism during chemical reactions: radical oxygen species (ROS) such as superoxide (O₂⁻), singlet oxygen (¹O₂), and hydroxyl radical (OH), as well as nitric oxide (NO), etc. They play an important role as regulatory mediators in signalling processes such as regulation of vascular tone, monitoring of oxygen tension in the control of ventilation and erythropoietin production and signal trans-

Abstract. Titanium dioxide (TiO₂) nanoparticles are extensively used today in sunscreens and coatings as protective compounds for human skin and material surfaces from UV radiation. In this paper, such particles are investigated by electron paramagnetic resonance spectroscopy as sources of free radicals under UV irradiation. The surface density of a placebo with embedded particles corresponds to the recommendations of dermatologists (2 mg cm⁻²). It is revealed that if applied onto glass, small particles 25 nm in diameter produce an increased amount of free radicals compared to the larger ones of 400 nm diam and the placebo itself. However, if applied onto porcine skin *in vitro*, there is no statistically distinct difference in the amount of radicals generated by the two kinds of particles on skin and by the skin itself. This proves that although particles as part of sunscreens produce free radicals, the effect is negligible in comparison to the production of radicals by skin *in vitro*. © 2009 Society of Photo-Optical Instrumentation Engineers. [DOI: 10.1117/1.3078802]

Keywords: titanium dioxide; nanoparticles; porcine skin; free radicals; ultraviolet light; phototoxicity.

Paper 08239SSR received Jul. 15, 2008; revised manuscript received Aug. 14, 2008; accepted for publication Aug. 22, 2008; published online Mar. 4, 2009.

duction from membrane receptors in various physiological processes.^{1,2} Under normal conditions, the amount of free radicals is balanced by enzymes and antioxidants. An excessive increase in ROS production is involved, for example, in the pathogenesis of cancer, diabetes mellitus, atherosclerosis, neurodegenerative diseases, rheumatoid arthritis, and ischemia/reperfusion injury.¹ The alien free radicals appear as a consequence of the effect of ionizing radiation, UV light, xenobiotics, etc. on human tissue and are harmful.

Studying of free radicals can be carried out by direct and indirect methods. The direct methods implement the effects of either electron paramagnetic resonance (EPR) or chemoluminescence. The indirect methods include investigations of the end products of the reactions with free radicals involved or application of inhibitors. The EPR (also called electron spin

Address all correspondence to A. P. Popov, M. V. Lomonosov Moscow State University, International Laser Center, Leninskie Gory, 119991, Moscow, Russia; Tel.: +7 (495) 939-2612; Fax: +7 (495) 939-3113; E-mail: dwelle@rambler.ru

resonance) technique is based on the absorption of microwave radiation by an unpaired electron of a molecule located in a magnetic field.

Direct detection of free short-living radicals by the EPR method is possible only at a quite low temperature (77 K, liquid nitrogen) due to their sufficient steady-state concentrations only under such conditions.³ In order to achieve suitable concentrations at room temperature, spin traps and spin markers are used (e.g., PCA, DPPH, Tempol, TEMPO, DMPO, 4-POBN). Spin traps are molecules which bind to short-lived free radicals and form detectable stable forms of radicals (spin adducts). Spin markers are stabilized radicals themselves contributing to the EPR signal; however, being in contact with short-lived free radicals, they loose or add an electron and become undetectable. The decrease in the EPR signal in this case quantifies the free radicals under investigation. The EPR methodology is a useful tool for the noninvasive *in vivo* measurements of skin barrier function, drug/skin interaction and cutaneous oxygen tension.³

Skin is a tissue protecting deeper-located organs from various hazards of the environment, such as chemical, biological, and physical hazards, in particular, from UV light. Exceeding doses of UV radiation can cause direct or indirect (via formation of free radicals) DNA damage, leading to carcinogenesis.⁴ Skin is a suitable object for EPR investigations due to its surface location and relatively small thickness. Using the microwave radiation of 1–10 GHz, which penetrates as deep as 1–35 mm into skin, it is possible to monitor penetration of spin traps and spin markers inside skin^{5,6} and in-depth appearance of generated radicals by means of EPR imaging.⁷ According to investigations, UV-induced radicals include ROS and lipid radicals^{8–10} as well as melanin radicals.¹¹ Formation of free radicals under UV irradiation and affect of various substances on this process in lipid-model systems^{12,13} of different complexity as *in vitro* counterparts of the intercellular lipid matrix of the stratum corneum was investigated by Trommer et al., in particular, using the EPR technique.¹² As shown by experiments with human skin *in vivo*,¹⁴ UVA part of the UV spectrum, is mainly responsible for the generation of free radicals (80–90% of the total amount) because of higher penetration depth, in contrast to UVB light, which contributes to radical generation only in the epidermis (up to a depth of 200 μm).

Titanium dioxide (TiO₂) nanoparticles are extensively used today in cosmetics, paints, air and water waste purification.¹⁵ Among three existing crystal modifications of TiO₂ (anatase, rutile, and brookite), anatase is the most photoactive, if irradiated by UV light, according to some authors.¹⁶ However, its photoactivity strongly depends on particle size, dopants,¹⁷ and coating and correlates with the reflectance spectra.¹⁸ Coatings are introduced to suppress photocatalytic properties of the particles.¹⁹ It is reported that both anatase and rutile particles used in sunscreens oxidize DNA and RNA *in vitro* and in human cell culture^{20–22} under UV irradiation. However, it is important to know whether the amount of radicals generated by the particles on skin exceeds that produced by the skin itself.

In this paper, we experimentally investigate the ability of titanium dioxide particles (anatase) of two average sizes (25 and 400 nm in diam) to produce free radicals under UV irra-

diation when applied to two different surfaces, glass and porcine skin *in vitro*.

2 Materials and Methods

Two types of commercially available samples were used in the experiments. A placebo (sunscreen o/w emulsion without any filters, Creme Sante soleil SPF 8 F148-006, RoC S.A., France) with coated titanium dioxide nanoparticles embedded was applied either onto glass slides or onto porcine skin *in vitro*. The surface density of the substance was 2 mg cm⁻², corresponding to the recommendations of COLIPA²³ for sunscreen applications. The placebo was weighted on precise-balance BP 211D (Sartorius, Göttingen, Germany) with an accuracy of 0.1 mg using a syringe. One type of spin marker, 3-carboxy-2,2,5,5-tetramethylpyrrolidine-1-oxyl (PCA, Sigma-Aldrich Chemie GmbH, Munich, Germany), was used to detect short-lived free radicals emerging under UV irradiation. PCA was dissolved from powder in a water-ethanol (1:1) solution at a concentration of 10 mM. It was chosen from other available spin markers due to satisfactory stability for our applications: after 3-min-long UV irradiation, the EPR signal decrease was ~1%, and after 18-min-long irradiation it was only 6%.²⁴ Additionally, in porcine skin there is a low amount of antioxidants, thus prolonging the existence on PCA. As a source of UV radiation (280–400 nm), a device TH-1E (Cosmedico Medizintechnik GmbH, Schwenningen, Germany) with the spectral maximum located at about 320 nm was used. The radiation intensity was 4.3 mW cm⁻², measured by the powermeter HBM-1 (Hydrosun Medizintechnik GmbH, Mullheim, Germany), which corresponds to the solar UV intensity (4.6 mW cm⁻²). The EPR system LBM MT 03 (Magnetech GmbH, Berlin, Germany) operating in L-band (1–1.5 GHz) was used for detecting the EPR signal. The generated short-lived radicals react with the nitrogen oxide PCA, which is thereby reduced to the corresponding hydroxylamine. PCA loses its free electron and the signal intensity in the EPR signal decreases.

2.1 Experiments with TiO₂ Nanoparticles Applied onto Glass Slides

Glass slides had the following dimensions: width 2.5 cm, length 5 cm, thickness 2 mm. There were three types of prepared slide samples (five couples of samples of each type): (i) placebo with small (25 nm) particles, (ii) placebo with large (400 nm) particles, and (iii) placebo only. Slides were covered homogeneously with a mixture of the corresponding substances (2 mg cm⁻²) and PCA (50 μL). In each couple, one sample was irradiated with the UV lamp (25-nm particles for 1 min, 400-nm particles and placebo only for 2 min); the other was used for control (was not irradiated). The samples were put into the EPR system and measured before and after the irradiation. The signals were displayed in real time on the computer screen in the software environment supplied with the system. They were stored as files and then analyzed.

2.2 Experiments with TiO₂ Nanoparticles Applied onto Porcine Skin

Native ears of domestic pigs were delivered from a nearby farm (Gut Hesterberg, Neurupin, Germany) on the day following the slaughter. Before the experiments, the ears were

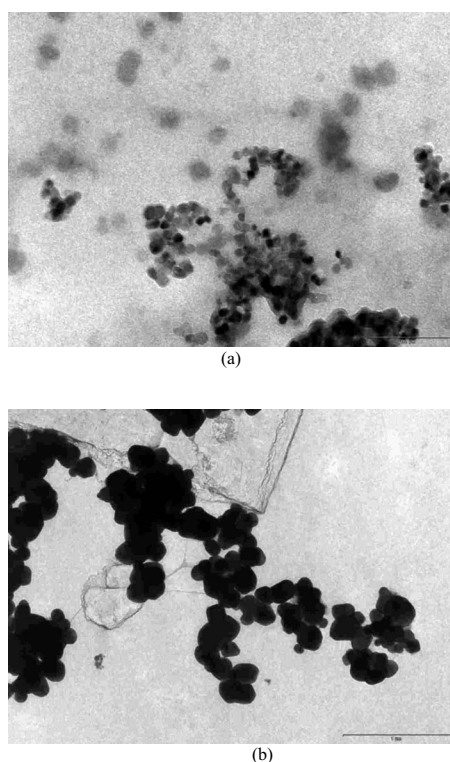


Fig. 1 TEM images of the 25- (a) and 400-nm (b) TiO₂ particles in a diluted placebo. Bars on the photographs correspond to 0.2 (a) and 1 μm (b). Magnification: 89 (a) and 22 (b).

washed with cold running water and gently wiped with paper napkins. All hairs on surfaces of the ears were completely removed with medical scissors with curved edges to avoid injuring the skin. Then, *tesa* adhesive tape (Beiersdorf AG, Hamburg, Germany) was used for tape stripping according to Weigmann et al.²⁵ Twenty tape strips were taken from the same area to remove the stratum corneum (horny layer, superficial layer of skin) in part. Corresponding to Ref. 26, such an amount of strips means that about 50% of stratum corneum was removed. A roller was used to press the tape to the skin. This procedure was a prerequisite to ease penetration of PCA into the skin.⁶ PCA served as a marker for revealing the production of free radicals. In the investigation of free radicals with the EPR technique, the deeper the PCA penetrated, the higher the amount of skin volume was involved. The surface of each porcine ear area, $5 \times 14 \text{ cm}^2$ in size, was marked with a permanent marker. The areas were divided into couples of small areas of 2.5×4 or $2.5 \times 3 \text{ cm}^2$. One area in the couple was used immediately after the preparation procedure was completed; the other area was used 25–30 min after the application of substances. The borders of all areas were covered by a color glue to build barriers between neighbouring areas. As in experiments with application of particles onto glass slides, three different substances were investigated: placebo with 25-nm particles, placebo with 400-nm particles, and placebo without particles. PCA was added to all substances (100 μL per each small area). The substances were topically applied onto the skin with a surface density of 2 mg cm^{-2} . During the application of the corresponding (according to the area) amount of the substances, the skin was massaged with a

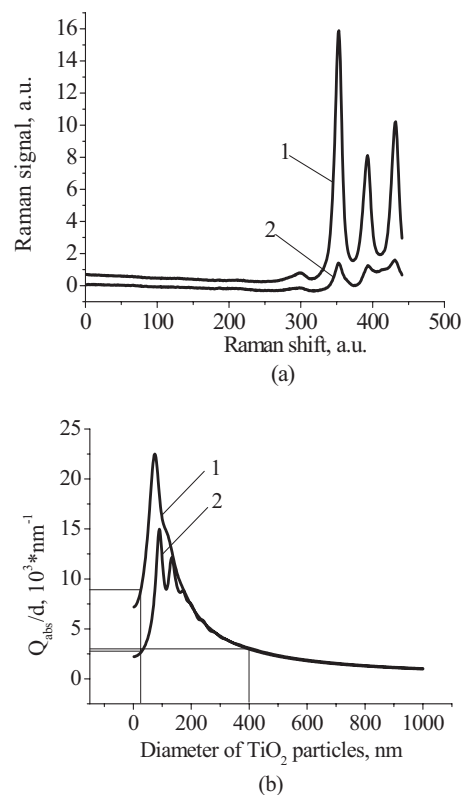


Fig. 2 Signal of Raman scattering (a) from powder titanium dioxide nanoparticles with diameters of 400 (1) and 25 nm (2); relative absorption efficiency factor (Q_{abs}/d) referred to the particle diameter for 310 (1) and 335-nm (2) UV radiation calculated according to the Mie theory; maxima of the curves correspond to the particle diameters of 74 and 90 nm (b).

massage device (Petra PC 60, petra-electric GmbH Co.KG) covered with a latex glove finger saturated in advance with the substance. From each small area, two punch biopsies were taken with a round-edged sharp cutter; one was later irradiated with the UV lamp (stratum corneum side), while the other was used for control. The diameter of the skin samples was 12 mm; the thickness was 2 mm (all skin layers from the surface to the cartilage in the middle of the ear). The biopsies were removed from the ear using a scalpel and pincers and were fixed onto a glass slide with acryl glue. Afterward, certain samples were irradiated by UV light for 3 min. The irradiated samples were measured in the EPR system before, immediately after and 15 min after the irradiation. Those serving as controls were measured at 0, 3, 7, 10, and 15 min (zero time corresponds to the start-time point of sample irradiation). Four to six samples were used for each measurement to collect statistical data.

2.3 Transmission Electron Microscopy (TEM)

TEM photos of particles were obtained using a transmission electron microscope Philips Morgagni 280 D (Eindhoven, the Netherlands).

2.4 Raman Spectroscopy

The Raman spectroscopy system (LMTB, Berlin, Germany)²⁷ was based on a CW Ar⁺ laser operating at the wavelength of

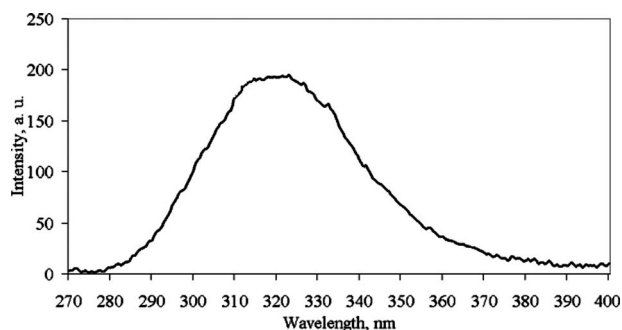


Fig. 3 Spectrum of the UV lamp used in the experiment.

514.5 nm (power 9 mW). Its radiation was focused into an optical fiber connected to an optical imaging system, where the light was filtered and focused onto samples. The Raman signal reflected from samples was collected by a lens system and transferred into another fiber bundle connected to a spectrograph. The spectrum was recorded by a charge-coupled device camera and transferred to a PC for processing. Because of flexibility of light delivering and collecting fibers, samples (TiO₂ particles as powder and imbedded in placebo) in cuvettes or applied onto glass slides were just put in contact with them. One measurement took a few seconds.

2.5 Mie Calculations

For Mie calculations, MieTab 7.23 software²⁸ was used. As input parameters, the radiation wavelength, refractive indices

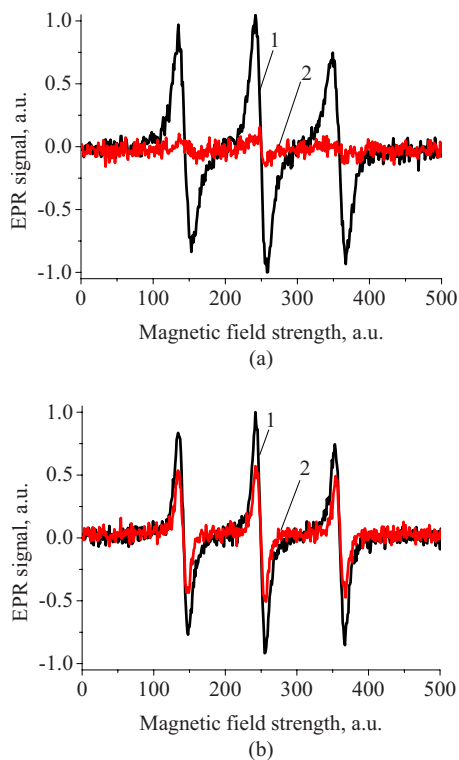


Fig. 4 EPR signals obtained from anatase 25-nm particles on glass (a) and on porcine skin (b) before (1) and after (2) UV irradiation. The samples on glass were irradiated for 1 min and the samples on skin for 3 min.

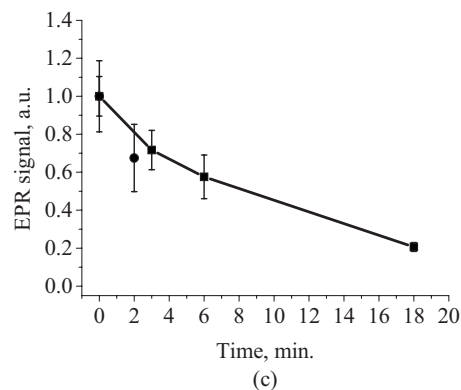
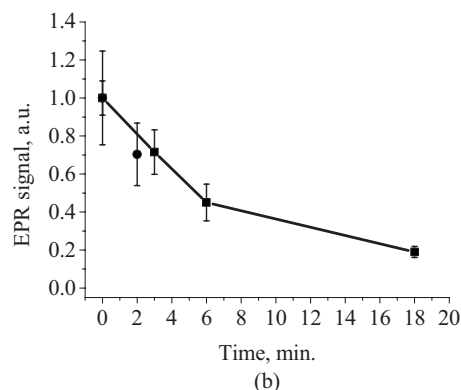
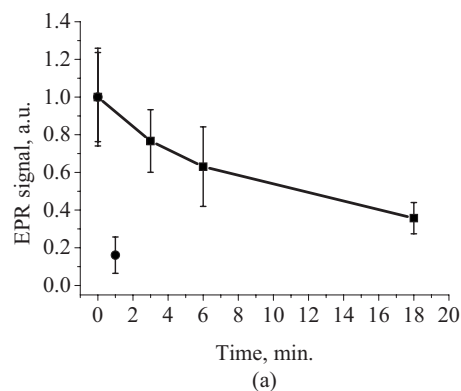


Fig. 5 Temporal dependences of amplitudes of the EPR signals obtained from the samples on glass: 25 (a) and 400-nm (b) particles and placebo without particles (c) UV-irradiated during 1 (a) or 2 min (b, c) (●) and not irradiated (■). Zero time corresponds to the beginning of UV irradiation (for the irradiated samples). For averaging, five samples of each type were measured.

of the particles and the surrounding medium, as well as particle sizes were required.

3 Results and Discussion

TEM photographs of the TiO₂ particles in diluted placebo are represented in Fig. 1. Magnification for the images of 25-nm particles was 89, while for 400-nm particles it was equal to 22. It is seen that the particles of both sizes form multiparticle structures. This process affects optical properties of the solutions.

In order to reveal the crystal form of the used titanium dioxide particles, we measured Raman spectra of the powder

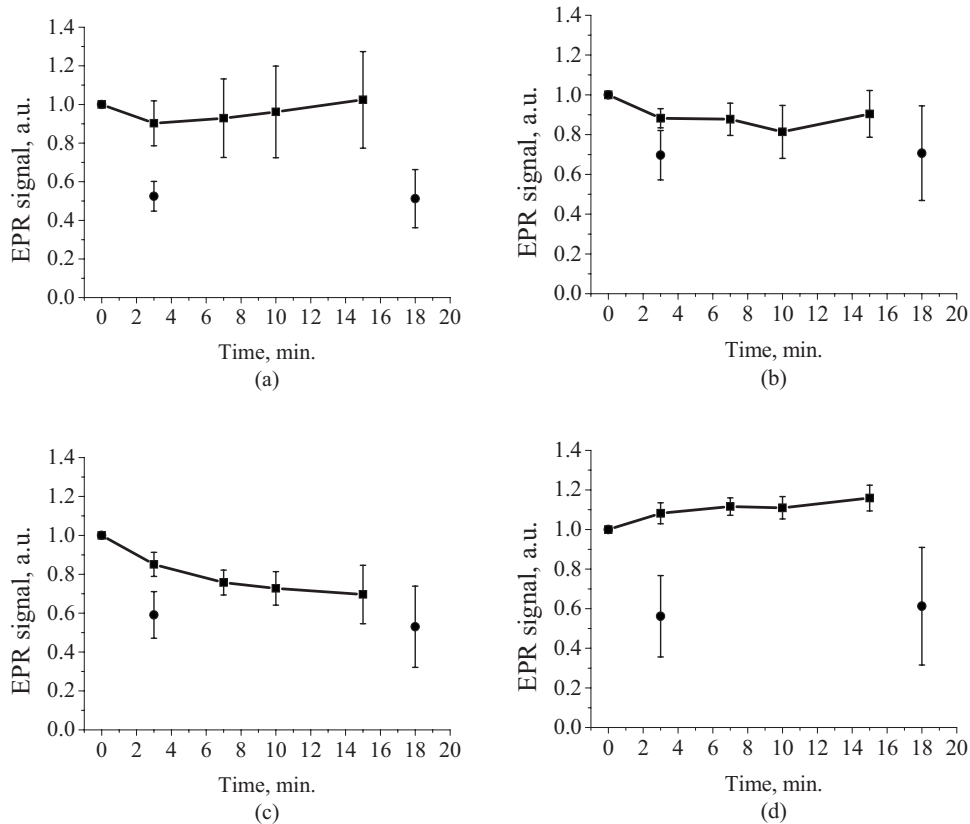


Fig. 6 Temporal dependences of amplitudes of the EPR signals obtained from the samples on porcine skin *in vitro* measured without 25–30-min-long delay: placebo with 25-nm particles (a), placebo with 400-nm (b) particles, placebo without particles (c), and skin without placebo and particles (d) UV-irradiated during 3 min (●) and not irradiated (■). For averaging, four skin samples with placebo and each type of the particles, six skin samples with placebo only, and six skin samples without placebo and particles were measured. Zero time corresponds to the beginning of UV irradiation (for the irradiated samples).

of particles and of the placebo with embedded particles. The obtained spectra are presented in Fig. 2(a). The signal produced by the placebo was much smaller than that of the powder due to a smaller concentration of particles (not shown). It is clearly seen that three peaks are present on the graph. This indicates, according to Ref. 29, that the crystal form of the particles under investigation is anatase.

The Mie theory was used to describe the interaction between the particles and UV radiation. The spectrum of the used UV light source is depicted in Fig. 3. For the calculations, two wavelengths were chosen: 310 and 335 nm. The first was chosen because it corresponds both to the maximum of the source spectrum and to the maximum of the product of the solar spectral irradiance over wavelength with the erythral action spectrum.³⁰ The second wavelength was taken for comparison; the anatase particles do not absorb light with a wavelength longer than 385 nm.³¹

Titanium dioxide is a birefringent crystal, with different refractive indices for light polarized perpendicular or parallel to the optic axis. In the “average index” approximation, the particles are supposed to be isotropic, with real and imaginary parts of the refractive index equal to $n_p = (2n_o + n_e)/3$ and $k_p = (2k_o + k_e)/3$, where n_o and k_o (n_e and k_e) are the ordinary (extraordinary) real and imaginary parts of the refractive index, respectively.³² For the 310- and 335-nm UV radiation, these constants taken from Ref. 31, result in: $n_p - ik_p = 3.48$

$-i 0.83$ (for 310 nm) and $n_p - ik_p = 3.37 - i 0.25$ (for 335 nm). The refractive index of the surrounding medium (placebo) was 1.4, and the diameters of the particles were considered to be 2–200 nm with 2-nm steps. The result of the calculation is shown in Fig. 2(b). Efficiency factor Q_{abs} is the ratio of the absorption and the geometrical cross sections of a particle. The value Q_{abs}/d , where d is a particle diameter, is proportional to the absorption coefficient of a particle suspension^{30,33–35} and therefore takes into account the presence of other particles of the same type in the sample.

Figure 4 illustrates typical signals obtained with the EPR system for the two investigated types of samples with 25-nm particles: located on glass and on porcine skin. The signals are normalized to the highest amplitude of the signal from the sample before irradiation. It is seen that after 1-min-long exposure to UV light the signal decreases. This means that short-lived free radicals appear.

Figure 5 shows the mean values with standard deviations of the results obtained from five samples on glass with or without particles. Standard deviations vary between 0.02 and 0.24 for nonirradiated samples and between 0.10 and 0.26 for the irradiated samples. Dependencies of the EPR signal on time for the irradiated and nonirradiated samples are depicted. Statistically, there is no effect of UV radiation in the presence of large particles and placebo without particles. However, the effect is distinctly seen in the case of small particles. This

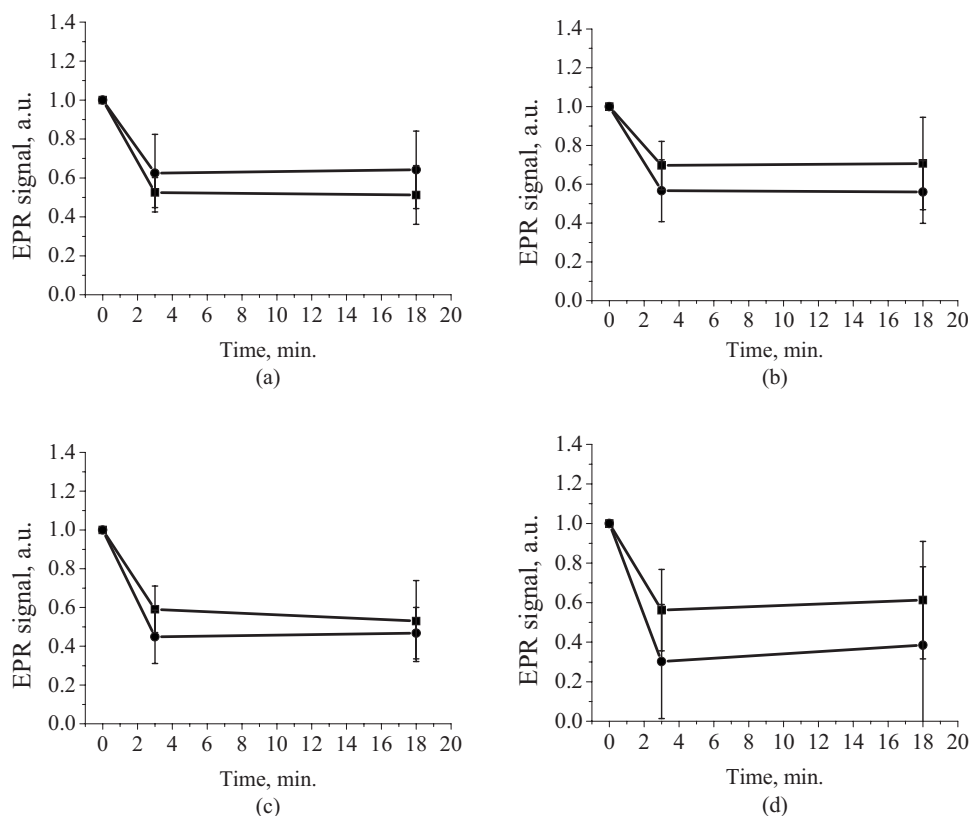


Fig. 7 Comparison of time-dependent amplitudes of the EPR signals after 3-min-long UV irradiation of the skin samples immediately after preparation (■) and 25–30 min later (●): placebo with 25-nm particles (a), placebo with 400-nm particles (b), placebo without particles (c), and skin without placebo and particles (d). For averaging, four skin samples with placebo and each type of the particles, six skin samples with placebo only, and six skin samples without placebo and particles were measured. Zero time corresponds to the beginning of UV irradiation (for the irradiated samples).

phenomenon can be explained in frames of the Mie theory. Considering Fig. 2(b) representing the absorption efficiency curves for 310- and 335-nm radiation, we can conclude that 25-nm particles absorb UV light much more efficiently than the 400-nm particles for $\lambda=310$ nm or at the same level for $\lambda=335$ nm at the same volume concentrations. As shown in Fig. 1, the particles form aggregates and agglomerates although ultrasonic stirring was used during the process of embedding particles into placebo. Formation of the above-mentioned structures causes an increase in the average size of particles, leading to the increased absorption efficacy of the 25-nm particles and decreasing that of the 400-nm particles. The larger absorption means more active production of free short-lived radicals. The curve corresponding to the nonirradiated large particles looks very similar to that of placebo and different from that of small particles.

The other series of experiments was carried out with porcine ear skin. One group of skin samples was irradiated immediately after preparation and the other with 25–30-min-long delay. The results of the measurements of the first group with standard deviations are presented in Fig. 6. Standard deviations vary between 0.04 and 0.25 for nonirradiated samples and between 0.08 and 0.30 for the irradiated samples. Taking into account the statistical errors, the effect of UV irradiation is clearly seen in all cases (the points corresponding to such samples are located lower than those of nonirra-

diated samples), and the magnitude of the effect is almost the same for the samples with the particles, with placebo only, and without placebo and particles. It means that the amounts of short-lived free radicals appearing under UV irradiation are comparable and do not depend on the presence of the particles on the skin surface. In other words, the contribution of skin to free-radical generation under UV irradiation exceeds that of the particles.

The effect of penetration time (0 versus 25–30 min) of the substances before UV irradiation is depicted in Fig. 7. There is no significant difference, but in the samples corresponding to large particles [Fig. 7(b)] as well as to the placebo [Fig. 7(c)] and to skin without placebo and particles [Fig. 7(d)], the lines connecting the average values relative to measurements without any delay are located above the lines corresponding to the delayed experiments. However, the situation is reverse for the samples with small particles [Fig. 7(a)].

4 Summary

As we proved experimentally by means of EPR spectroscopy, small (25 nm in diam) nanoparticles of titanium dioxide (anatase form) are more photoactive than large (400 nm in diam) particles. This effect is clearly seen if the particles embedded into the placebo are applied on glass and is in agreement with the Mie theory. However, if the particles are applied onto the

porcine skin *in vitro*, no distinct difference is observed. This is caused by high skin contribution to the generation of radicals. In comparison to the skin's ability to produce radicals, the nanoparticles do not play a significant role in the concentrations used (2 mg cm⁻²).

Acknowledgments

The authors thank Dr. Maxim Darvin for his assistance during the experiments and Dr. Elena Zagainova from Nizhny Novgorod Medical Academy (Russia) for the TEM photos of the particles. A.P.P. thanks Infotech Oulu and the Tauno Tönning Foundation (both Finland) and DAAD (Germany) for support of this study. This work was partially supported by the RFBR Grant No. 07-02-01000.

References

1. W. Dröge, "Free radicals in the physiological control of cell function," *Physiol. Rev.* **82**, 47–95 (2002).
2. D. Darr and I. Fridovich, "Free radicals in cutaneous biology," *J. Invest. Dermatol.* **102**, 671–675 (1994).
3. J. Fuchs, T. Herrling, and N. Groth, "Detection of free radicals in skin: a review of the literature and new developments," in *Oxidants and Antioxidants in Cutaneous Biology*, J. Thiele and P. Elsner, Editors, Vol. **29**, pp. 1–17, Karger, Basel (2001).
4. H. N. Ananthaswamy and W. E. Pierceall, "Molecular mechanisms of ultraviolet radiation carcinogenesis," *Photochem. Photobiol.* **52**, 1119–1136 (1990).
5. T. Herrling, J. Fuchs, and N. Groth, "Kinetic measurements using EPR imaging with a modulated field gradient," *J. Magn. Reson.* **154**, 6–14 (2002).
6. M. Meinke, S. Haag, N. Groth, F. Klein, R. Lauster, W. Sterry, and J. Lademann, "Method for detection of free radicals in skin by EPR spectroscopy after UV irradiation," *SÖFW-J.* **134**, 2–11 (2008).
7. T. Herrling, K. Jung, and J. Fuchs, "Measurements of UV-generated free radicals/reactive oxygen species (ROS) in skin," *Spectrochim. Acta, Part A* **63**, 840–845 (2005).
8. J. Nishi, R. Ogura, M. Sugiyama, T. Hidaka, and M. Kohno, "Involvement of active oxygen in lipid peroxide radical reaction of epidermal homogenate following ultraviolet light exposure," *J. Invest. Dermatol.* **97**, 115–119 (1991).
9. R. Ogura, M. Sugiyama, J. Nishi, and N. Haramaki, "Mechanism of lipid formation following exposure of epidermal homogenate to ultraviolet light," *J. Invest. Dermatol.* **97**, 1044–1047 (1991).
10. T. Herrling, J. Fuchs, J. Rehberg, and N. Groth, "UV-induced free radical in the skin detected by ESR spectroscopy and imaging using nitroxides," *Free Radic Biol. Med.* **35**, 59–67 (2003).
11. B. Collins, T. O. Poehler, and W. A. Bryden, "EPR persistence measurements of UV-induced melanin free radicals in whole skin," *Photochem. Photobiol.* **62**, 557–560 (1995).
12. H. Trommer, R. Böttcher, A. Pöpl, J. Hoentsch, S. Wartewig, and R. H. H. Neubert, "Role of ascorbic acid in stratum corneum lipid models exposed to UV irradiation," *Pharmacol. Res.* **19**, 982–990 (2002).
13. H. Trommer and R. H. H. Neubert, "Screening for new antioxidative compounds for topical administration using skin lipid model systems," *J. Pharm. Pharm. Sci.* **8**, 494–506 (2005).
14. T. Herrling, L. Zastrow, J. Fuchs, and N. Groth, "Electron spin resonance detection of UVA-induced free radicals," *Skin Pharmacol. Appl. Skin Physiol.* **15**, 381–383 (2002).
15. U. Diebold, "The surface science of titanium dioxide," *Surf. Sci. Rep.* **48**, 53–229 (2003).
16. L. Cao, A. Huang, F.-J. Spiess, and S. L. Suib, "Gas-phase oxidation of 1-butene using nanoscale TiO₂ photocatalysts," *J. Catal.* **188**, 48–57 (1999).
17. Z. Zhang, C.-C. Wang, R. Zakaria, and J. Y. Ying, "Role of particle size in nanocrystalline TiO₂-based photocatalysts," *J. Phys. Chem. B* **102**, 10871–10878 (1998).
18. A. V. Vorontsov, A. A. Altyinnikov, E. N. Savinov, and E. N. Kurkin, "Correlation of TiO₂ photocatalytic activity and diffuse reflectance spectra," *J. Photochem. Photobiol., A* **144**, 193–196 (2001).
19. J. Lademann, H.-J. Weigmann, H. Schaefer, G. Mueller, and W. Sterry, "Investigation of the stability of coated titanium microparticles used in sunscreens," *Skin Pharmacol. Appl. Skin Physiol.* **13**, 258–264 (2000).
20. H. Hidaka, S. Horikoshi, N. Serpone, and J. Knowland, "In vitro photochemical damage to DNA, RNA and their bases by an inorganic sunscreen agent on exposure to UVA and UVB radiation," *J. Photochem. Photobiol., A* **111**, 205–213 (1997).
21. R. Dunford, A. Salinaro, L. Cai, N. Serpone, S. Horikoshi, H. Hidaka, and J. Knowland, "Chemical oxidation and DNA damage catalysed by inorganic sunscreen ingredients," *FEBS Lett.* **418**, 87–90 (1997).
22. W. G. Warner, J.-J. Yin, and R. R. Wei, "Oxidative damage to nucleic acids photosensitized by titanium dioxide," *Free Radic Biol. Med.* **23**, 851–858 (1997).
23. COLIPA, European Cosmetic, Toiletry and Perfumery Association, "COLIPA sun protection factor test method," Ref. 94/289 (1994).
24. S. Haag, *Nachweis von freien Radikalen in biologischen Proben mittels ESR-Spektroskopie*, Diploma, Technical University Berlin, Berlin (2007).
25. H.-J. Weigmann, J. Lademann, H. Meffert, H. Schaefer, and W. Sterry, "Determination of the horny layer profile by tape stripping in combination with optical spectroscopy in the visible range as a prerequisite to quantify percutaneous absorption," *Skin Pharmacol. Appl. Skin Physiol.* **12**, 34–45 (1999).
26. A. P. Popov, J. Lademann, A. V. Priezzhev, and R. Myllylä, "Reconstruction of stratum corneum profile of porcine ear skin after tape stripping using UV/VIS spectroscopy," *Proc. SPIE* **6628**, 66281S-1–6 (2007).
27. M. E. Darvin, I. Gersonde, M. Meinke, W. Sterry, and J. Lademann, "Noninvasive *in vivo* determination of the carotenoids beta-carotene and lycopene concentrations in the human skin using the Raman spectroscopic method," *J. Phys. D* **38**, 2696–2700 (2005).
28. MieTab is a Mie scattering program for Microsoft Windows (<http://amiller.nmsu.edu/mietab.html>) (published October 15, 2004; last accessed June 20, 2008).
29. K. D. O. Jackson, "A guide to identifying common inorganic fillers and activators using vibrational spectroscopy," *Internet J. Vib. Spectros.* **3** (1998) (<http://www.ijvs.com/volume2/edition3/section3.html#ackson>).
30. A. P. Popov, A. V. Priezzhev, J. Lademann, and R. Myllylä, "TiO₂ nanoparticles as effective UV-B radiation skin-protective compound in sunscreens," *J. Phys. D* **38**, 2564–2570 (2005).
31. G. E. Jellison, Jr., L. A. Boatner, and J. D. Budai, "Spectroscopic ellipsometry of thin film and bulk anatase (TiO₂)," *J. Appl. Phys.* **93**, 9537–9541 (2003).
32. B. R. Palmer, P. Stamatakis, C. F. Bohren, and G. C. Salzman, "A multiple scattering model for opacifying particles in polymer films," *J. Coat. Technol.* **61**, 41–47 (1989).
33. A. P. Popov, J. Lademann, A. V. Priezzhev, and R. Myllylä, "Effect of size of TiO₂ nanoparticles embedded into stratum corneum on UVA and UVB sun-blocking properties of the skin," *J. Biomed. Opt.* **10**, 064037-1-9 (2005).
34. A. P. Popov, A. V. Priezzhev, J. Lademann, and R. Myllylä, "The effect of nanometer particles of titanium oxide on the protective properties of skin in the UV region," *J. Opt. Technol.* **73**, 208–211 (2006).
35. A. P. Popov, A. V. Priezzhev, J. Lademann, and R. Myllylä, "Effect of multiple light scattering by titanium dioxide nanoparticles implanted into a superficial skin layer on radiation transmission in different wavelength regions," *Quantum Electron.* **37**, 17–21 (2007).